Hexaplatinum Clusters with Carbonyl and Diphosphine Ligands and the Trapping of Mercury(0) and Thallium(I)

Leijun Hao, Jagadese J. Vittal, and Richard J. Puddephatt*

Department of Chemistry, University of Western Ontario, London, Ontario, Canada N6A 5B7

Received February 28, 1996[⊗]

Hexaplatinum cluster complexes have been prepared by reduction of $[PtCl_2(SMe_2)_2]$ with $NaBH_4$ in the presence of CO and the diphosphine ligands $Ph_2P(CH_2)_nPPh_2$, $n = 2$ (dppe), 3 (dppp), 4 (dppb), 5 (dpppe), and 6 (dpph). The products are the closed cluster $[Pt_6(\mu\text{-}CO)_6(\mu\text{-dppe})_3]$, **2b**, and the open cluster $[Pt_6(\mu\text{-}CO)_6(\mu\text{-dppp})_2(dppp)_2]$, **9**, but the reactions failed to give isolable products when $n = 4-6$. Cluster **9** can encapsulate mercury(0) or thallium(I) with loss of dppp to give the closed clusters $[Pt_6(\mu_6\text{-Hg})(\mu\text{-}CO)_6(\mu\text{-dppp})_3]$, **10a**, or $[Pt_6(\mu_6\text{-Tl})(\mu\text{-}CO)_6(\mu\text{-dppp})_3]^+$, **11a**, respectively. The $Pt_6(\mu\text{-}CO)_6(\mu\text{-dppp})_3$ unit acts as a cryptand and evidence is presented that the cluster **10a** must open to allow reaction with thallium(I) to give **11a**. Reduction of $[PtCl_2(SMe_2)_2]$ with $NaBH_4$ in the presence of CO, the diphosphine ligands $Ph_2P(CH_2)_nPPh_2$, and mercury can give $[Pt_6(\mu_6\text{-Hg})(\mu\text{-}CO)_6\{\mu\text{-}Ph_2P(CH_2)_nPPh_2\}_3]$, **10a**−**d**, $n = 3-6$, respectively, directly, but clusters $[Pt_6(\mu_6\text{-Hg})(\mu\text{-}CO)_6(CO)_2\{\mu\text{-}Ph_2P(CH_2)_n\text{-}PPh_2\}_2]$, **12**, are also formed in some cases. Cluster **2b** reacts with $[Ph_3PAu]^+$ to give $[Pt_6(\mu\text{-}CO)_6(\mu\text{-dppe})_3(\mu_3\text{-}AuPPh_3)_2]^{2+}$.

Introduction

The encapsulation of a metal ion by a cryptand ligand has dramatic effects on both the thermodynamic stability and kinetic reactivity of the resulting cryptate complex since the metal ion is physically trapped and cannot easily escape.[1] This article describes a study of the synthesis of cluster cryptate complexes, in which two trinuclear platinum clusters of the type $[Pt_3(\mu\text{-}CO)_3L_3]$, **1**,[2] are held together by using bidentate phosphine ligands LL of the type $Ph_2P(CH_2)_nPPh_2$ to give $[\{Pt_3(\mu\text{-}CO)_3\}_2(\mu\text{-LL})_3]$, **2** (Chart 1). If n is large enough, the space between the clusters should be great enough to encapsulate a guest metal atom or ion. In related research, the electrochemical reduction at a mercury electrode of a platinum(II) precursor in the presence of a diphosphine and an isocyanide ligand has been studied in detail.[3,4] Among a rich diversity of products were the complexes $[Pt_6(Hg_n)(\mu\text{-CNR})_6(RNC)_2(\mu\text{-LL})_2]$ [**3**, $n = 1$, LL = dppb; **4**, $n = 2$, LL = dpppe, dpph] and $[Pt_6(Hg_2)(\mu\text{-CNR})_6(\mu\text{-LL})_3]$ (**5**, LL = dpppe, dpph) (Chart 1).[3] Synthetic reactions could be carried out using sodium amalgam as reducing agent in some cases.[3] Since the reactions must be carried out in the presence of mercury, only the mercury inclusion complexes could be isolated, and no mercury inclusion complexes were detected when the shorter methylene chain diphosphines dppm, dppe, and dppp were used; other interesting Pt−Pt-bonded binuclear and trinuclear complexes were formed instead (Chart 1, complexes **6**−**8**).[3,4] Following earlier studies of the cluster $[Pt_6(\mu\text{-}CO)_6(\mu\text{-dppm})_3]$, **2a**,[5] it was of interest to determine if analogous carbonyl clusters with longer methylene chain diphosphines could be synthesized and if they might display interesting inclusion chemistry as the space between the Pt_3 triangles in **2** increased. The reducing agent used was $Na[BH_4]$, since it can yield mercury-free com-

Chart 1[a]

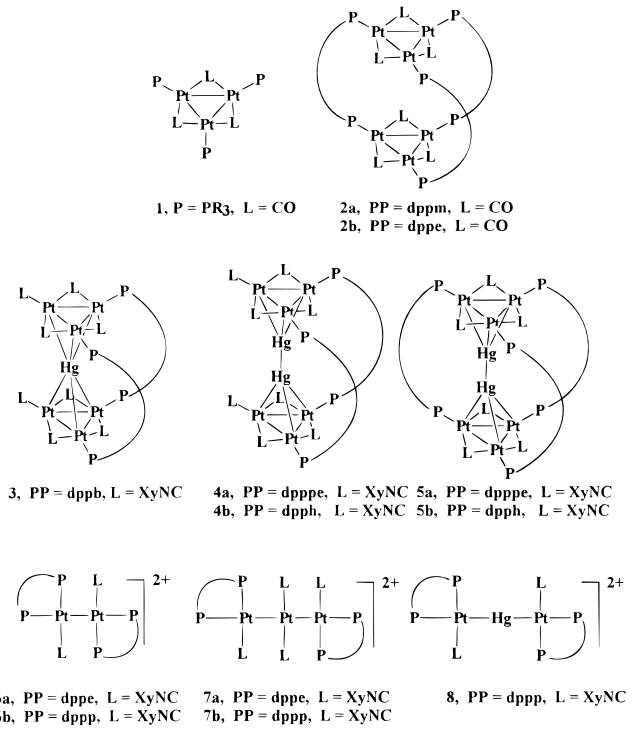

[a] Complex **8** was originally formulated ad $[Pt\{Pt(PP)L\}_2]^{2+}$ in ref 3.

[⊗] Abstract published in *Advance ACS Abstracts,* June 15, 1996.

(1) (a) Lehn, J.-M. *Angew. Chem., Int. Ed. Engl.* **1988**, *27*, 89. (b) Mertes, K. B.; Lehn, J.-M. In *Comprehensive Organometallic Chemistry*; Wilkinson, G., Ed.; Pergamon: Oxford, U.K., 1987; Vol. 2, Chapter 21.3. (c) Muller, A.; Reuter, H.; Dillinger, S. *Angew. Chem., Int. Ed. Engl.* **1995**, *34*, 2328.

(2) For reviews, see: (a) Imhof, D.; Venanzi, L. M. *Chem. Soc. Rev.* **1994**, 185. (b) Cross, R. J. In *Comprehensive Organometallic Chemistry*, 2nd ed.; Pergamon: Oxford, U.K., 1995; Vol. 9, Chapter 7. (c) Mingos, D. M. P.; Wardle, R. W. M. *Transition Met. Chem.* **1985**, *10*, 441.

(3) Tanase, T.; Ukaji, H.; Kudo, Y.; Ohno, M.; Kobayashi, K.; Yamamoto, Y. *Organometallics* **1994**, *13*, 1374.

(4) Tanase, T.; Horiuchi, T.; Yamamoto, Y.; Kobayashi, K. *J. Organomet. Chem.* **1992**, *440*, 1.

(5) (a) Hao, L.; Spivak, G. J.; Xiao, J.; Vittal, J. J.; Puddephatt, R. J. *J. Am. Chem. Soc.* **1995**, *117*, 7011. (b) Spivak, G. J.; Hao, L.; Vittal, J. J.; Puddephatt, R. J. *J. Am. Chem. Soc.* **1996**, *118*, 225.

S0276-7333(96)00148-3 CCC: $12.00

plexes.[5,6] A preliminary account of the chemistry with the ligand dppp has been published.[7]

Results

A Hexanuclear Cluster with Bis(diphenylphosphino)ethane, dppe. Reduction of $[PtCl_2(SMe_2)_2]$ with $NaBH_4$ in the presence of CO and dppe led directly to the closed cluster $[Pt_6(\mu\text{-}CO)_6(\mu\text{-dppe})_3]$, **2b**, which was isolated as a red-brown solid which was slowly decomposed on exposure to air. The cluster was characterized spectroscopically by comparison to the well-known clusters $[Pt_3(\mu\text{-}CO)_3(PR_3)_3]$, **1**.[2] The IR spectrum contained only bridging carbonyl bands at $\nu(CO) = 1840$ (m), 1796 (vs), 1780 (vs, sh), and 1731 (s) cm^{-1}, in the same region as found for **1**.[2] The ^{31}P NMR spectrum of **2b** is also similar to those reported for **1**.[2] It contained only a singlet at $\delta(^{31}P) = 53.2$, with satellites showing the couplings $^1J(PtP) = 4814$ Hz, $^2J(PtP) = 527$ Hz, and $^3J(PP) = 64$ Hz. No coupling $^3J(PCH_2CH_2P)$ and no long range $^{195}Pt^{31}P$ coupling between triangles was observed. In ^{13}C-enriched samples, the bridging carbonyl ligands gave a single resonance in the ^{13}C NMR at $\delta(^{13}C) = 248.1$ which appeared as a 1:8:18:8:1 quintet due to the coupling $^1J(PtC) = 709$ Hz, this intensity pattern being characteristic of a $Pt_2(\mu_2\text{-}CO)$ ligand.[2] In the presence of free ^{13}CO, this resonance broadened and the ^{195}Pt satellite spectra were lost, indicating easy exchange between free and coordinated CO at room temperature. No long-range $^{195}Pt^{13}C$ coupling was resolved. The ^{31}P NMR spectrum was not affected by the presence of free CO, indicating that no adducts between **2b** and CO are formed in significant amounts. The NMR spectra of **2b** were essentially unchanged at −90 °C, indicating that the apparent high symmetry is probably not a function of fluxionality. All evidence therefore indicates that **2b** has the proposed structure and that there is little Pt···Pt bonding between the two triangles.[5]

A Hexanuclear Cluster with Bis(diphenylphosphino)propane, dppp. Reduction of $[PtCl_2(Me_2S)_2]$ with excess $NaBH_4$ in the presence of dppp = $Ph_2P(CH_2)_3PPh_2$ and CO gave the new cluster complex $[Pt_6(\mu\text{-}CO)_6(\mu\text{-dppp})_2(dppp)_2]$, **9**, Chart 2, in 85% yield as a brown-red solid. Cluster **9** can be considered to contain two separate Pt_3 clusters bridged by two μ-dppp ligands, and it is therefore an analog of the known trinuclear complexes $[Pt_3(\mu\text{-}CO)_3L_4]$[2] and in particular of the dppp derivative $[Pt_3(\mu\text{-}CO)_3(PCy_3)_2(dppp)]$.[8] The IR and room-temperature NMR data for **9** and $[Pt_3(\mu\text{-}CO)_3(PCy_3)_2(dppp)]$[8] are very similar, and so **9** was readily characterized by spectroscopic methods as outlined below. At room temperature, the NMR spectra indicate an effective plane of symmetry containing all platinum atoms, the carbonyl ligands, and phosphorus atoms of the μ-dppp ligands and bisecting the chelating dppp ligands. Thus, for example, only two ^{31}P resonances of equal intensity are observed, one due to the bridging [$\delta(^{31}P) = 56.5$, $^1J(PtP) = 4682$ Hz, $^2J(Pt^1P) = 534$ Hz, $^2J(Pt^2P) = 445$ Hz, $^3J(P^bP^{b'}) = 60$ Hz, $^3J(P^aP^b) = 19$ Hz] and one

Chart 2

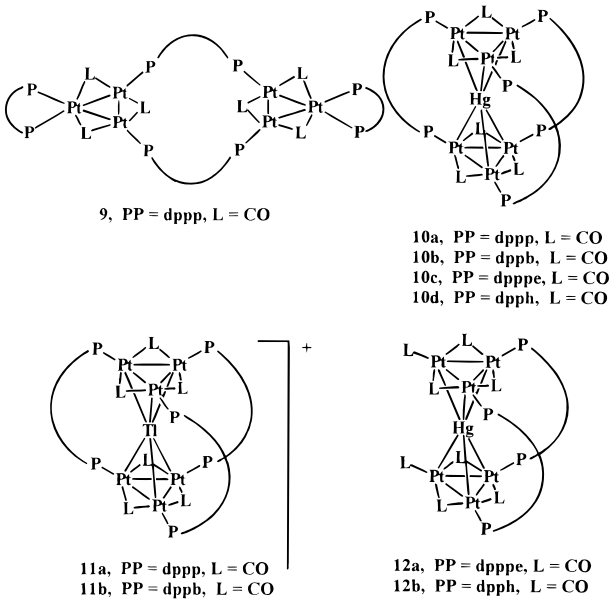

to the chelating [$\delta(^{31}P) = 25.5$, $^1J(PtP) = 3425$ Hz, $^2J(PtP) = 294$ Hz, $^3J(P^aP^b) = 19$ Hz] dppp ligands. The ^{13}C NMR spectrum contained two resonances due to the carbonyls C^1O [$\delta(^{13}C) = 233.2$, $^1J(Pt^2C^1) = 790$ Hz, $^1J(Pt^1C^1) = 628$ Hz, $^2J(Pt^2C^1) = 24$ Hz] and C^2O [$\delta(^{13}C) = 256.1$, $^1J(Pt^2C^2) = 791$ Hz]. Finally, the ^{195}Pt NMR spectrum contained two resonances, due to the nonequivalent atoms Pt^1 [$\delta(^{195}Pt) = -2220$, $^1J(Pt^1P^a) = 3425$ Hz, $^2J(Pt^1P^b) = 536$ Hz, $^1J(Pt^1Pt^2) = 386$ Hz] and Pt^2 [$\delta(^{195}Pt) = -2424$, $^1J(Pt^2P^b) = 4682$ Hz, $^2J(Pt^2P^{b'}) = 445$ Hz, $^2J(Pt^2P^a) = 290$ Hz, $^1J(Pt^1Pt^2) = 386$ Hz]. The major coupling $^1J(PtP)$ gave rise to a triplet for Pt^1 and a doublet for Pt^2, thus immediately confirming the number of directly bonded phosphorus atoms. These spectra clearly define the structure **9**, having effective D_{2h} symmetry.

However, at low temperature, two resonances are observed in the ^{31}P NMR spectrum for the phosphorus atoms of the chelating dppp ligand. This is clearly a result of fluxionality and shows that the true symmetry of **9** is lower than D_{2h}, probably C_{2v} or C_2. There are two reasonable explanations. First, it is probable that the structure is not planar but angular, and the fluxionality might then involve angular to planar to angular equilibration as shown in the upper part of Scheme 1. Second, it is possible that the structure is effectively planar but that the coordination of the chelating dppp ligand is equatorial−axial and that the fluxionality involves equatorial−axial exchange as shown in the lower part of Scheme 1. Of course, some combination of both processes is also possible.

The open structure **9** is clearly favored over the closed structure **2**, and attempts to prepare **2**, with LL = dppp, have been unsuccessful. For example, if a deficiency of dppp is used during the reduction of $[PtCl_2(SMe_2)_2]$, **9** is still the only detected product with some of the precursor being reduced to metallic platinum.

Hexanuclear Clusters with Diphosphine Ligands dppb, dpppe, and dpph. The analogous reactions to those described above were unsuccessful in these cases. For example, in the reduction with dppb a red-brown solid was obtained which gave $\nu(CO)$ at 1995 and 1790 cm^{-1}, indicating the presence of both terminal and

(6) (a) Dahmen, K. H.; Moor, A.; Naegeli, R.; Venanzi, L. M. *Inorg. Chem.* **1991**, *30*, 4285. (b) Holah, D. G.; Hughes, A. N.; Krysa, E.; Magnuson, V. R. *Organometallics* **1993**, *12*, 4721.

(7) Hao, L.; Vittal, J. J.; Puddephatt, R. J. *Inorg. Chem.* **1996**, *35*, 269.

(8) (a) Hallam, M. F.; Howells, N. D.; Mingos, D. M. P.; Wardle, R. W. M. *J. Chem. Soc., Dalton Trans.* **1985**, 845. (b) Briant, C. E.; Wardle, R. W. M.; Mingos, D. M. P. *J. Organomet. Chem.* **1984**, *267*, C49.

Scheme 1. Possible Mechanisms of Fluxionality

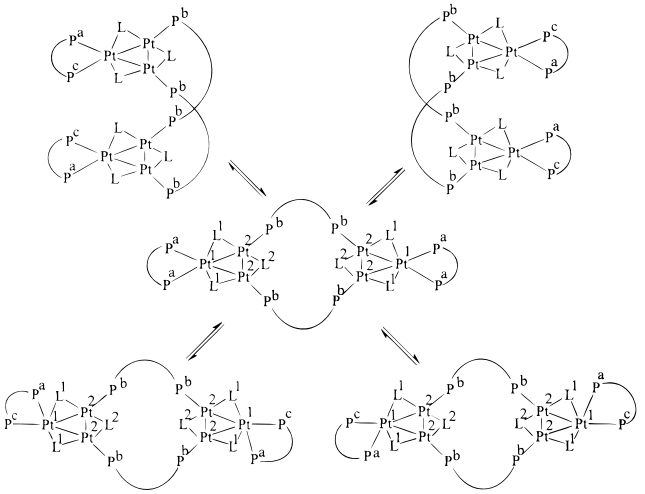

bridging carbonyl ligands. In the ^{31}P NMR spectrum, there were very broad resonances at $\delta = 35$ and 50 and a sharper resonance at $\delta = 17$, and no ^{195}Pt satellites were resolved either at room temperature or at −90 °C in dichloromethane solution. The nature of these cluster complexes, including the question of whether or not they are homogeneous, is therefore still unknown. They are clearly platinum(0) clusters as shown by the reaction chemistry described below.

Trapping Reactions with Mercury(0) and Thallium(I). Attempts to prepare clusters containing mercury(0) or thallium(I) were made either by direct reaction with the above clusters or by carrying out the reduction of $[PtCl_2(SMe_2)_2]$ in the presence of CO, the diphosphine ligand, and Hg(0) or Tl(I).

No pure adducts of **2b** with mercury(0) or thallium(I) could be obtained by the above methods. For example, when mercury was added to a solution of **2b** in CD_2Cl_2, the ^{31}P NMR spectrum after 2 h showed that no reaction had occurred, though a change in color was observed. After 2 days, much decomposition had occurred but no mercury adduct was detected by ^{31}P NMR. Molecular modeling shows that the cavity in **2b** is too small to accommodate a central mercury(0) atom or thallium(I) ion, and so complex formation would either occur at an external face or by opening up of the cluster. Neither appears to give rise to pure clusters.

With the longer chain diphosphines, mercury(0) or thallium(I) inclusion is possible and gives rise to stable complexes. This is clearly illustrated by the reaction of **9** with mercury(0) or Tl[PF_6], which occurs with loss of 1 equiv of dppp to form the closed carcerand clusters **10a** or **11a**, respectively (Scheme 2). These reactions occur rapidly and quantitatively. In this sense, the open cluster **9** acts as a kind of "Venus flytrap" since, once the heavy metal is complexed and the third μ-dppp ligand is in place, the incarcerated metal cannot easily escape. This is demonstrated by attempted metal-for-metal replacement reactions. Thus, addition of mercury to **11a** gives no reaction after either 1 h or 1 day (some decomposition occurs over 1 day). Addition of Tl[PF_6] to **10a** gives no reaction after 1 h but about 20% **11a** is formed after 1 day (along with some decomposition); the reaction is accelerated in the presence of free dppp and significant conversion of **10a** to **11a** is observed after 1 h under these conditions. Quantitative kinetic studies

Scheme 2

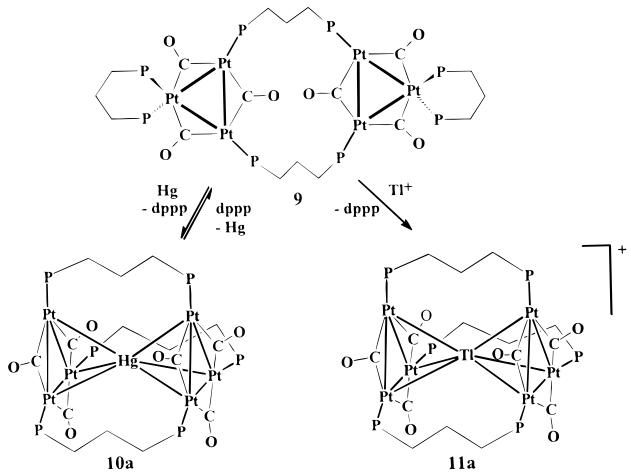

Table 1. Selected NMR (ppm, Hz) and IR Data (cm^{-1}) for the Closed Pt_6 Clusters

	2a[a]	**2b**	**10a**	**11a**	**10b**	**11b**	**10c**	**10d**
$\delta(^{31}P)$	37.6	53.2	58.6	56.7	46.6	47.0	53.2	52.9
$^1J(PtP)$	5289	4814	5037	4810	4919	5040	4987	4961
$^2J(PtP)$	274	527	403	360	396	*c*	403	397
$^3J(PP)$	*b*	64	55	50	56	*c*	55	56
$\delta(^{13}CO)$	240.5	251	235	232.5	238	236	235	233
$^1J(PtC)$	757	697	714	696	715	705	720	744
$\nu(CO)$	1790	1840	1837	1871	1864	1808	1830	1823
	1773	1796	1799	1818	1828	1776	1788	1781
		1780	1782		1802			
		1731			1791			

[a] From ref 5. [b] A broad doublet splitting of 216 Hz is probably due to $^2J(PP)$. [c] Broad spectrum, not resolved. Complete data are in the experimental section.

are not possible due to the general decomposition which competes with the desired reaction, but it is immediately obvious that the conversion of **10a** to **11a** is much slower than the conversion of **9** to **11a**. It is proposed that direct loss of mercury from **10a** is impossible and that opening up of one of the μ-dppp bridges (aided by free dppp) must occur prior to the metal for metal exchange, as shown schematically in Scheme 2. Complex **10a** was also prepared directly by the reduction of $[PtCl_2(SMe_2)_2]$ in the presence of CO, dppp, and excess mercury.

The complexes **10a** and **11a** were characterized spectroscopically, and **11a**[BPh_4] was also characterized by an X-ray structure determination. Each complex gave a single resonance in the ^{31}P NMR spectrum due to the diphosphine ligands and in the ^{13}C NMR due to the bridging carbonyl ligands, thus confirming the high symmetry of the products (Table 1). Complex **10a** gave a single resonance in the ^{195}Pt NMR which appeared as a doublet due to $^1J(PtP) = 5037$ Hz, clearly indicating that there is just one phosphorus atom bound to each platinum. The metal−metal couplings were $^1J(HgPt) = 3350$ Hz, $^1J(PtPt) = 2200$ Hz, and $^2J(PtPt) = 100$ Hz. The coupling $^1J(HgPt)$ is smaller, and $^1J(PtPt)$ is larger than in the related clusters $[Pt_3(\mu\text{-}CO)_3L_3(\mu_3\text{-}HgX)_2]$ (L = phosphine, X = halide), for which the ranges are $^1J(HgPt) = 5784-6723$ Hz and $^1J(PtPt) = 1609-1860$ Hz, respectively.[9] The ^{31}P NMR spectrum of **11a** was broader than for **10a**, and the weaker satellite peaks needed to extract PtPt and PtTl couplings were not fully

(9) Albinati, A.; Dahmen, K. H.; Demartin, F.; Forward, J. M.; Longley, C. J.; Mingos, D. M. P.; Venanzi, L. M. *Inorg. Chem.* **1992**, *31*, 2223.

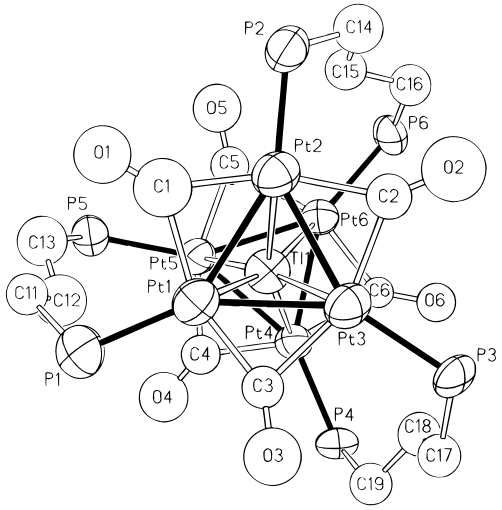

Figure 1. View of the structure of the cluster cation **11a**. The closest intertriangle Pt···Pt distance is Pt(2)Pt(6) = 5.036(3) Å, which is clearly nonbonding. The angle between the planes Pt(1)Pt(2)Pt(3) and Pt(4)Pt(5)Pt(6) is 2.0(1)°.

Table 2. Selected Bond Distances (Å) and Angles (deg) in 11a[BPh_4]

Tl(1)−Pt(1)	2.860(3)	Tl(1)−Pt(4)	2.909(3)
Tl(1)−Pt(3)	2.920(3)	Tl(1)−Pt(2)	2.942(3)
Tl(1)−Pt(5)	2.967(3)	Tl(1)−Pt(6)	2.992(3)
Pt(1)−Pt(2)	2.682(3)	Pt(1)−Pt(3)	2.673(3)
Pt(2)−Pt(3)	2.667(3)	Pt(4)−Pt(5)	2.677(3)
Pt(4)−Pt(6)	2.658(3)	Pt(5)−Pt(6)	2.666(3)
Pt(1)−P(1)	2.23(2)	Pt(2)−P(2)	2.25(2)
Pt(3)−P(3)	2.25(1)	Pt(4)−P(4)	2.25(1)
Pt(5)−P(5)	2.27(1)	Pt(6)−P(6)	2.25(1)
Pt(1)−C(3)	1.91(4)	Pt(1)−C(1)	2.11(6)
Pt(2)−C(1)	2.02(5)	Pt(2)−C(2)	2.03(4)
Pt(3)−C(3)	2.08(4)	Pt(3)−C(2)	2.08(5)
Pt(4)−C(4)	1.95(4)	Pt(4)−C(6)	2.02(4)
Pt(5)−C(5)	2.00(4)	Pt(5)−C(4)	2.06(5)
Pt(6)−C(6)	1.98(4)	Pt(6)−C(5)	2.15(4)
Pt(1)−Tl(1)−Pt(4)	136.5(1)	Pt(1)−Tl(1)−Pt(3)	55.08(7)
Pt(4)−Tl(1)−Pt(3)	121.29(9)	Pt(1)−Tl(1)−Pt(2)	55.03(7)
Pt(4)−Tl(1)−Pt(2)	165.3(1)	Pt(3)−Tl(1)−Pt(2)	54.12(7)
Pt(1)−Tl(1)−Pt(5)	124.32(9)	Pt(4)−Tl(1)−Pt(5)	54.20(6)
Pt(3)−Tl(1)−Pt(5)	173.9(1)	Pt(2)−Tl(1)−Pt(5)	131.4(1)
Pt(1)−Tl(1)−Pt(6)	168.2(1)	Pt(4)−Tl(1)−Pt(6)	53.52(7)
Pt(3)−Tl(1)−Pt(6)	128.91(9)	Pt(2)−Tl(1)−Pt(6)	116.5(1)
Pt(5)−Tl(1)−Pt(6)	53.15(6)	Pt(3)−Pt(1)−Pt(2)	59.74(8)
Pt(3)−Pt(1)−Tl(1)	63.60(8)	Pt(2)−Pt(1)−Tl(1)	64.04(8)
Pt(3)−Pt(2)−Pt(1)	59.97(8)	Pt(3)−Pt(2)−Tl(1)	62.52(8)
Pt(1)−Pt(2)−Tl(1)	60.93(8)	Pt(2)−Pt(3)−Pt(1)	60.29(8)
Pt(2)−Pt(3)−Tl(1)	63.36(8)	Pt(1)−Pt(3)−Tl(1)	61.32(7)
Pt(6)−Pt(4)−Pt(5)	59.96(8)	Pt(6)−Pt(4)−Tl(1)	64.83(8)
Pt(5)−Pt(4)−Tl(1)	63.99(8)	Pt(6)−Pt(5)−Pt(4)	59.67(8)
Pt(6)−Pt(5)−Tl(1)	63.91(7)	Pt(4)−Pt(5)−Tl(1)	61.81(7)
Pt(4)−Pt(6)−Pt(5)	60.38(8)	Pt(4)−Pt(6)−Tl(1)	61.65(8)
Pt(5)−Pt(6)−Tl(1)	62.94(7)		

resolved. However, the presence of thallium was clearly shown by the doublet appearance of the central resonance due to ^2J(TlP) = 335 Hz. Attempts to obtain a ^{195}Pt NMR spectrum of **11a** were unsuccessful, but **11a** was characterized structurally. A view of the cation is given as Figure 1 and selected bond distances and angles are given in Table 2.

The six platinum atoms have a geometry intermediate between the trigonal prism and antiprism [the dihedral angles typified by P(1)Pt(1)Pt(5)P(5) and P(1)Pt(1)Pt(4)P(4) fall in the ranges 32.4−34.4° and −79.0 to −86.8°; ideal values would be 0 and −120° for the trigonal prism and 60 and −60° for the trigonal antiprism]. The Pt−Pt distances within each Pt_3 triangle are in the range 2.658(3)−2.682(3) Å, well within the range found for Pt−Pt single bonds in related clusters,[2−13] but the intertriangle Pt···Pt distances are greater than 5 Å and so are clearly nonbonding. The thallium atom is bonded in sandwich fashion to all six platinum atoms with Pt−Tl distances in the range 2.860(3)−2.992(3) Å. There are no other Pt_6Tl clusters for comparison, but the related cluster $[Pt_3(\mu_3\text{-Tl})(\mu\text{-CO})_3(PCy_3)_3]^+$ has Pt−Tl = 3.034(1)−3.047(1) Å, *longer* than in **11a**.[11] It is relevant to note that the mean angles PtPC, PCC, and CCC for the dppp ligands in **11a** are 113, 113, and 114°, respectively, all greater than the ideal tetrahedral angle, suggesting that the dppp ligands are stretched slightly in order to span the two Pt_3 triangles whose centroids are separated by 4.98 Å. Perhaps there is a balance between these two effects and the PtTl distances are slightly smaller than their ideal values in **11a** to minimize this stretching of the dppp ligands.

In the case of the longer chain diphosphine ligands, the mercury inclusion complexes **10** were best prepared by reduction of $[PtCl_2(SMe_2)_2]$ in the presence of CO and the corresponding diphosphine dppb, dpppe, or dpph, followed by addition of excess mercury. In the case of dppb, the complex **10b** was prepared in high yield by use of the stoichiometric amount of dppb. However, in the other cases, formation of **10c** (dpppe) or **10d** (dpph) was accompanied by formation of **12**, which are analogous to the known isocyanide cluster **3**. The clusters **12** could not be isolated in pure form, and their identification is based primarily on NMR and IR data of their mixtures with **10**. In addition, reaction of **12** with more diphosphine occurred easily to give **10** by displacement of the terminal carbonyl ligands (eq 1) and the clusters **10** could then be isolated in analytically pure form.

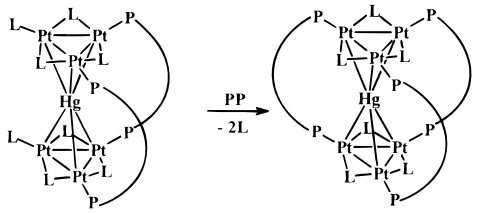

(1)

12a, PP = dpppe, L = CO
12b, PP = dpph, L = CO
10c, PP = dpppe, L = CO
10d, PP = dpph, L = CO

The NMR data for **10b**−**d** are similar to those for **10a** discussed earlier and clearly define the symmetrical $Pt_6(\mu\text{-CO})_6(\mu\text{-PP})_3$ unit (Table 1). The platinum−diphosphine−carbonyl skeleton of **12** is also clearly defined. Thus, a ^{13}CO-enriched sample of **12a** gave three carbonyl resonances in the ^{13}C NMR spectrum, and the characteristic chemical shifts and ^1J(PtC) couplings define one terminal CO resonance, one unsymmetrical μ_2-CO resonance [2 × $Pt^1Pt^2(\mu\text{-CO})$], and one symmetrical μ_2-CO resonance [$Pt^2{}_2(\mu\text{-CO})$] at each Pt_3 triangle. The ^{31}P NMR spectrum contained a singlet, with three sets of ^{195}Pt satellites on either side due to isotopomers containing a single ^{195}Pt atom,

(10) Yamamoto, Y.; Yamazaki, H.; Sakurai, T. *J. Am. Chem. Soc.* **1982**, *104*, 2329.
(11) Ezomo, O. J.; Mingos, D. M. P.; Williams, I. D. *J. Chem. Soc., Chem. Comm.* **1987**, 924.
(12) Yamamoto, Y.; Yamazaki, H. *Inorg. Chim. Acta* **1994**, *217*, 121.
(13) Schoettel, G.; Vittal, J. J.; Puddephatt, R. J. *J. Am. Chem. Soc.* **1990**, *112*, 6400.

appearing as two doublets due to $^1J(\mathrm{Pt^2P})$ and $^2J(\mathrm{Pt^{2'}P})$, with the doublet splitting due to $^3J(\mathrm{PP})$, and a singlet due to $^2J(\mathrm{Pt^1P})$. In the ^{195}Pt NMR spectrum of **12a**, only the Pt^1 resonance was observed and it appeared as a 1:8:18:8:1 quintet of 1:2:1 triplets, as a result of the couplings $^1J(\mathrm{Pt^1Pt^2})$ and $^2J(\mathrm{Pt^1P})$, respectively. For **12b**, both ^{195}Pt resonances were observed, the Pt^1 resonance being sharp and the Pt^2 resonance very broad with only the $^1J(\mathrm{PtP})$ coupling resolved. No ^{199}Hg satellites were resolved for either **12a** or **12b**.

The chief problem in characterizing **10b**−**d** and **12a**−**b** is the determination of the number of mercury atoms present. In the analogous isocyanide clusters, there is one mercury present when LL = dppb in **3** but two when LL = dpppe or dpph in **4**.[4] It was therefore surprising to find that the C,H analyses for all complexes **10b**−**d** indicated the presence of only one mercury atom. The ratio of Pt:Hg was then determined by energy dispersive X-ray (EDX) analysis on crystalline samples, and each gave a Pt:Hg ratio of 6:1, as expected for structure **10**, but clearly inconsistent with the presence of two mercury atoms in each cluster. There is a marked difference between the stoichiometries of the otherwise similar μ-CO and μ-CNR cluster complexes.[4] Since the clusters **12** were not obtained in analytically pure form, their composition is less certain and a structure with two mercury atoms is not excluded.

The thallium sandwich cluster **11b** was prepared by reduction of $[\mathrm{PtCl_2(SMe_2)_2}]$ in the presence of CO, dppb, and thallium(I), but the similar reactions with longer chain diphosphines dpppe and dpph failed to give pure clusters. The ^{31}P NMR spectrum of **11b** was particularly broad, and no fine structure was observed, except for the satellites due to $^1J(\mathrm{PtP})$. Otherwise the characterization was similar to that described for **11a**.

Addition of $\mathrm{Ph_3PAu^+}$ to 2b. Since it was argued that **2b** could not incorporate a mercury atom because the space between the two $\mathrm{Pt_3}$ triangles was too small, the question arose as to whether or not external complexation might occur. No reaction occurred with mercury(0). However, the reagent $\mathrm{Ph_3PAu(thf)^+}$, prepared by reaction of $\mathrm{Ph_3PAuCl}$ with $\mathrm{AgPF_6}$ in tetrahydrofuran, reacted with **2b** to give $[\mathrm{Pt_6(\mu\text{-}CO)_6(\mu\text{-}dppe)_3(\mu_3\text{-}AuPPh_3)_2}][\mathrm{PF_6}]_2$, **13**, according to eq 2. This reaction

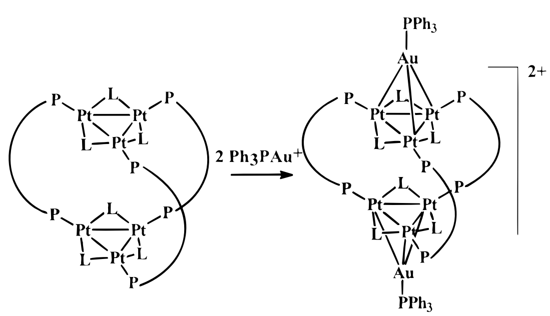

(2)

2b, PP = dppe, L = CO	13, PP = dppe, L = CO

is analogous to the known reaction with the trinuclear clusters **1** and shows that **2b** is electron rich.[8] The ^{31}P NMR spectra at both room temperature and at −90 °C contained singlet resonances for the $\mathrm{Ph_3PAu}$ groups and for the dppe ligands, as expected for **13**. The triply bridging nature of the $\mathrm{AuPPh_3}$ groups is shown by the intensities of the satellites due to the long-range coupling $^2J(\mathrm{PtAuP})$.[8] This coupling was observed only in the low-temperature NMR spectrum and indicates easy exchange of the $\mathrm{PPh_3}$ ligands or easy reversible dissociation of the $\mathrm{Ph_3PAu^+}$ groups.

Neither complex **9** nor **10a**−**d** gave pure products on reaction with $\mathrm{Ph_3PAu^+}$. Thus, encapsulation of a mercury atom appears to reduce the tendency to form a stable adduct with the electrophile $\mathrm{Ph_3PAu^+}$.

Discussion

This work has shown that cluster cryptands can be prepared based on the triangular platinum clusters $[\mathrm{Pt_3(\mu\text{-}CO)_3(PR_3)_3}]$ by substituting diphosphine ligands $\mathrm{Ph_2P(CH_2)_nPPh_2}$ for the monodentate phosphines. There are similarities but also major differences between these clusters and those based on the unit $[\mathrm{Pt_3(\mu\text{-}CNXy)_3(PR_3)_3}]$, where Xy = 2,6-dimethylphenyl.[3,4] A trend can be seen in which the two $\mathrm{Pt_3}$ triangles tend to be closer together for the μ-CO than for the μ-CNXy clusters. Thus, for the isocyanide clusters, there is no analog of **2b** or of **10a** perhaps because steric hindrance between XyNC ligands would prevent the necessary close approach of the two $\mathrm{Pt_3}$ triangles. A slightly different argument is needed to rationalize why there is no XyNC analog of **10b** (reaction of **3** with dppb failed to give the closed cryptand cluster).[4] The $\mathrm{(CH_2)_4}$ chain would allow a greater distance between $\mathrm{Pt_3}$ triangles, but if there is only space for one mercury atom, the $\mathrm{Pt_3}$ triangles still need to be about 5 Å apart to allow PtHg bonding to both triangles. Similarly, the dpppe and dpph ligands give **5**, containing two mercury atoms, for the XyNC system but **10**, containing only one Hg atom, for the CO system. Naturally, the $\mathrm{Pt_3}$ triangles will be much further apart in **5** and so the problem of steric hindrance between μ-XyNC groups is eliminated.

The bonding in the clusters **10** and **11** is of interest. First consider the experimental evidence of the carbonyl stretching frequencies. For complexes with μ-dppp ligands, the values of ν(CO) are **2b** ~ **10a** < **11a** (note that **2** does not exist with dppp ligands so the closest analog with dppe ligands is chosen for comparison). These data indicate that mercury is neither a net donor nor acceptor with respect to the $\mathrm{Pt_3}$ triangles but that $\mathrm{Tl^+}$ is a net acceptor. Thus as charge is donated from the $\mathrm{Pt_3}$ triangle to $\mathrm{Tl^+}$ there is correspondingly less back-bonding to the bridging carbonyl ligands and the observed frequencies ν(CO) are higher. Within the series of mercury-encapsulated clusters, the sequence is ν(CO) for **10a** < **10b** > **10c** > **10d**, but the range of values is small and the significance of the series is not clear.

Next consider isolobal analogies. The frontier donor orbitals of a $\mathrm{Pt_3}$ triangle have a + e symmetry, and so the $\mathrm{Pt_3}$ triangle can be considered isolobal with $\mathrm{C_5H_5^-}$.[14] Hence the complexes **10** and **11** can be considered isolobal to $\mathrm{Cp_2Hg^{2-}}$ (unknown) or $\mathrm{Cp_2Tl^-}$.[15] Now salts of $\mathrm{Cp_2Tl^-}$ have an angular structure with a stereochemically active lone pair of electrons on thallium(I), although high-level MO calculations indicate that the linear structure is only slightly higher in energy.[15] In the structure of **11**, the $\mathrm{Pt_3}$ triangles are constrained to

(14) Xiao, J.; Hao, L.; Puddephatt, R. J.; Manojlović-Muir, Lj.; Muir, K. W. *J. Am. Chem. Soc.* **1995**, *117*, 6316.

(15) Armstrong, D. R.; Herbst-Irmer, R.; Kuhn, A.; Moncrieff, D.; Paver, M. A.; Russell, C. A.; Stalke, D.; Steiner, A.; Wright, D. S. *Angew. Chem., Int. Ed. Engl.* **1993**, *32*, 1774.

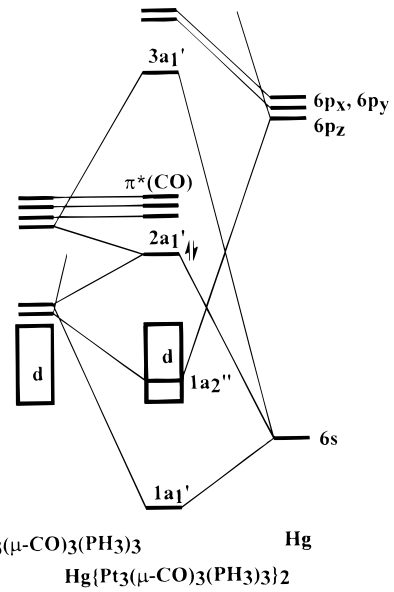

Figure 2. Simplified energy correlation diagram for formation of $[Hg\{Pt_3(\mu\text{-}CO)_3(PH_3)_3\}_2]$ from $\{Pt_3(\mu\text{-}CO)_3(PH_3)_3\}_2$ and a Hg atom. Complications due to mixing of the Pt−Pt bonding MO's with d-levels and mixing of Pt p_z with π^*(CO) orbitals are not shown for the sake of clarity.

be almost parallel by the presence of the three μ-dppp ligands, but the Tl atom is actually slightly displaced from the ideal position between the centroids of the Pt_3 triangles toward Pt(1), Pt(3), and Pt(4) (distances Pt−Tl = 2.860, 2.920, and 2.909 Å, respectively) and away from Pt(2), Pt(5), and Pt(6) (distances Pt−Tl = 2.942, 2.967, and 2.992 Å, respectively). The distortion is small, and it is not clear if it arises to minimize repulsions with the lone pair on thallium(I). EHMO calculations were carried out on the model clusters $[M\{Pt_3(\mu\text{-}CO)_3(PH_3)_3\}_2]^{n+}$, ($n$ = 0, M = Hg; n = 1, M = Tl), in order to gain further insight.

First, calculations were carried out for geometries between the trigonal prism and trigonal antiprism while keeping all bond distances constant. The energy was marginally lower for the trigonal antiprism but by only 0.04 eV, and there was very little barrier to rotation of the Pt_3 triangles. The stereochemistry adopted by such sandwich clusters in the solid state is therefore likely to be determined by steric and packing factors. The geometry of **11a** is intermediate between the two idealized structures, but most calculations were carried out in the trigonal prismatic structure with D_{3h} symmetry for simplicity. A simplified energy correlation diagram for formation of the mercury cluster is given in Figure 2. It is convenient to discuss the bonding in terms of the interactions of the mercury 6s orbital (filled) and 6p orbitals (empty) with the platinum cluster orbitals, whose nature has been discussed extensively in earlier publications.[2,16]

The 6s orbital interacts with the symmetrical combination of Pt_3 bonding MO's of a_1' symmetry (mixed with combinations of orbitals of same symmetry having d_{z^2} and d_{xz}, d_{yz} character to improve overlap) to give bonding and antibonding combinations $1a_1'$ and $2a_1'$, respectively (Chart 3, **A**, **B**). Since both orbitals are filled, this would normally be unfavorable. However, there is also overlap of the mercury 6s orbital with empty cluster MO's

(16) Mingos, D. M. P.; Slee, T. *J. Organomet. Chem.* **1990**, *394*, 679.

Chart 3

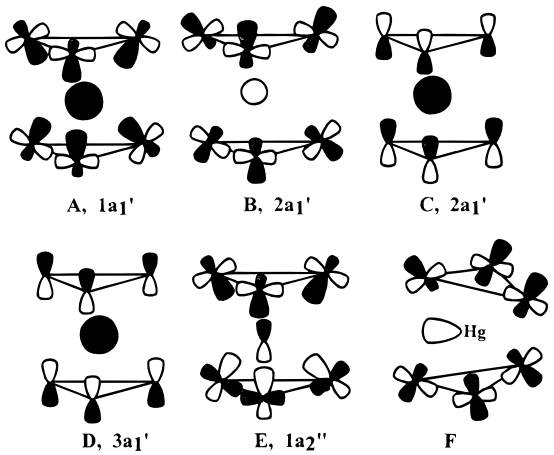

having platinum p_z and carbonyl π^* character. $2a_1'$ has bonding character in this respect while $3a_1'$ is antibonding (Chart 3, **C**, **D**; note that the CO ligands and orbital contributions are omitted for the sake of simplicity). Thus it is the mercury 6s to platinum $6p_z$ overlap that leads to a net bonding interaction between mercury and platinum, and this transfers charge from mercury to platinum.

A bonding interaction of comparable magnitude occurs by overlap of the filled unsymmetrical combination of Pt_3 bonding MO's of a_2'' character (again mixed with more d_{z^2} and d_{xz}, d_{yz} character for better overlap) with the empty mercury $6p_z$ orbital (Chart 3, **E**). There is weaker π-overlap of several filled orbitals having platinum 5d-character and e′ symmetry with the empty mercury $6p_x$, $6p_y$ orbitals. Both effects lead to charge transfer from platinum to mercury.

Both the MO calculations (charge on mercury +0.05 e) and carbonyl stretching frequencies (see above discussion) suggest that the two bonding effects are about equal, and so there is very little net transfer of electron density from mercury to platinum. As the charge on the central metal increases in the series Hg(0) to Tl(I) to the hypothetical Pb(II), the corresponding 6s and 6p orbitals will move to lower energy and the charge transfer from the Pt_3 clusters to the central metal 6p orbitals will increase while the reverse 6s to Pt_3 charge transfer will decrease, but otherwise, of course, there are strong similarities. The lower contribution of the 6s versus 6p bonding accounts for the higher values of ν(CO) for the thallium(I) complex. Our efforts to prepare the isoelectronic Pb(II) cluster complex have been unsuccessful.

In all cases, the calculations indicate that the orbital $2a_1'$ is at relatively high energy and that the HOMO−LUMO gap is relatively small, the HOMO having Pt−Pt bonding but Pt−M antibonding character and the LUMO having mostly CO π^* character. It is the small HOMO−LUMO gap which gives rise to the unusual blue or green colors of **10** or **11**. The orbital $2a_1$ is mostly localized on the platinum clusters and has relatively little 6s character of the central metal. Two consequences may be envisioned. First, it may be possible to oxidize the clusters by two electrons, for example to give the mercury(II) analog with the orbital $2a_1'$ vacant. We note in this respect that the isoelectronic gold(I) cluster $[Au\{Pt_3(\mu\text{-}CO)_3L_3\}_2]^+$, L = PPh_3,

Table 3. Atomic Charge on the Central Metal M [Z(M)/e] and Pt−M and Pt−Pt Overlap Populations from EHMO Calculations on Pt_6M^n = $[Pt_6(\mu_6\text{-}M)(\mu\text{-}CO)_6(PH_3)_6]^n$

CVE[a]	cluster	Z(M)	OP(Pt−M)	OP(Pt−Pt)
96	Pt_6Au^-	0.02	0.11	0.18
94	**Pt_6Au^+**	**0.17**	**0.12**	**0.17**
96	**Pt_6Hg^0**	**0.05**	**0.16**	**0.17**
94	Pt_6Hg^{2+}	0.18	0.17	0.15
96	**Pt_6Tl^+**	**0.95**	**0.16**	**0.16**
94	Pt_6Tl^{3+}	1.06	0.18	0.15
96	Pt_6Pb^{2+}	1.83	0.18	0.16
94	Pt_6Pb^{4+}	1.89	0.20	0.14

[a] This gives the cluster valence electron (CVE) counts, counting 12e and 10e for M^n having electron configurations $5d^{10}6s^2$ and $5d^{10}$, respectively. If the $5d^{10}$ electrons are considered core electrons, the corresponding electron counts would be 86 and 84. The entries in bold correspond to known complexes. In the calculations, the distances Pt−M and Pt−Pt are constant at 2.84 and 2.63 Å, respectively.

is already known.[17] Perhaps the auride ion Au^- might be stabilized by two-electron reduction in this case. Results from the EHMO calculations for 96-electron ($2a_1'$ filled) and 94-electron clusters ($2a_1'$) vacant are given in Table 3. Note that, for each central metal M, the charge on M increases only 0.06−0.15 e on going from the 96e to 94e cluster, as expected if the orbital $2a_1$ has relatively little M character, and that the Pt−M and Pt−Pt overlaps are higher and lower, respectively, for the 94e clusters. The data in Table 3 do suggest that, perhaps when M = Au or Hg where the charges are not excessive, both 96e and 94e clusters might be prepared. Unfortunately, the $Pt_3(\mu\text{-}CO)_3$ units are not very robust and chemical oxidation/reduction has not given isolable products. Electrochemical studies would be valuable for further study. It is noteworthy that the mean Pt−Pt and Pt−M distances are slightly shorter and considerably longer for the 96e **11a** [mean Pt−Pt = 2.670, Pt−Tl = 2.931 Å] compared to the 94e cluster $[Au\{Pt_3(\mu\text{-}CO)_3L_3\}_2]^+$, L = PPh_3 [mean Pt−Pt = 2.683, Pt-Au = 2.728 Å],[17] respectively, as expected if the $2a_1'$ MO is Pt−Pt bonding but Pt−M antibonding. Second, there is still a question of whether the "linear" or "angular" $M(Pt_3)_2$ units is intrinsically more stable. In the real complexes, the linear structures are probably necessary on steric grounds, but the smaller substituents in the model compounds allow a theoretical study. To minimize steric effects on going to the angular structure, we have used the staggered trigonal antiprism as the base structure and then changed the angle between the centroids of the Pt_3 triangles and the central mercury(0) or thallium(I) atom from 180° through to 150°. The calculations do indicate that the HOMO is stabilized by this deformation as the "lone pair" has less antibonding character (compare **B** and **F**, Chart 3). However, this effect is more than offset by several other minor but unfavorable changes and the calculations indicate that the linear structure is most stable (the calculated energy difference is about 0.3 eV for a 20° distortion).

In conclusion, the linear $M(Pt_3)_2$ structure appears to be preferred for metal atoms or ions M with both the $5d^{10}$ and $5d^{10}6s^2$ electron configurations and easy redox reactions between these states may be predicted. Optimum stability of the cryptand clusters $[M\{Pt_3(\mu\text{-}CO)_3(\mu\text{-}Ph_2P(CH_2)_xPPh_2)_3]^{n+}$ containing a single "guest" atom or ion M^{n+} appears to occur when the bridging diphosphine is dppp or dppb (x = 3 or 4).

Experimental Section

All reactions were carried out under N_2 atmosphere using Schlenk techniques. The compound $[PtCl_2(Me_2S)_2]$ was prepared by the literature method.[18] IR spectra were recorded by using a Perkin-Elmer 2000 spectrometer; the NMR spectra were recorded by using a Varian Gemini-300 spectrometer. The proton and carbon chemical shifts are referenced to external Me_4Si, and $^{31}P\{^1H\}$ and $^{195}Pt\{^1H\}$ NMR spectra are externally referenced to 85% H_3PO_4 and a saturated D_2O solution of K_2PtCl_4.

EDX analyses were conducted for **10**, **11**, and **13**. The results showed that the ratio Pt:Hg = 6 in **10a**−**d**, Pt:Tl = 6 in **11a**,**b**, and Pt:Au = 3:1 in **13**.

$[Pt_6(\mu\text{-}CO)_6(\mu\text{-}dppe)_3]$, 2b. To a solution of $[PtCl_2(Me_2S)_2]$ (210 mg, 0.527 mmol) in THF (80 mL) was added dppe (105 mg, 0.27 mmol). CO was bubbled through the solution 20 min, and excess $NaBH_4$ (279 mg) was then added to the stirred solution. The color of the solution changed through yellow-green, green, dark green, and finally to deep red over ca. 1 h. After 8 h of stirring under a steady CO flow, MeOH (20 mL) was added dropwise and effervescence occurred. The color of the solution turned to bright red. The solution was allowed to stir overnight under a CO atmosphere, and a deep red-purple solution was obtained. The solvent was then removed by vacuum, and the red-purple residue was extracted with CH_2Cl_2 (20 mL × 8), the solution was filtered through Celite to remove suspended material, and the solvent was evaporated to give the product as a brown-red solid in 80% yield. Well-shaped crystals could be obtained from CH_2Cl_2/diethyl ether or CH_2Cl_2/hexane. Anal. Calcd for $C_{84}H_{72}O_6P_6Pt_6$: C, 39.8; H, 2.9. Found: C, 40.2; H, 2.4. IR (Nujol): ν(CO) = 1840 (m), 1796 (vs), 1780 (vs, sh), 1731 (s) cm^{-1}. NMR in CD_2Cl_2 at 22 °C: $\delta(^1H)$ = 3.43 [s, br, 12H, C***H₂***C***H₂*** of μ-dppe]; $\delta(^{13}C)$ = 246.6 [s, br, μ-***C***O] in the presence of free ^{13}CO; after removal of excess CO, $\delta(^{13}C)$ = 248.1 [quintet, 1:8:18:8:1, ^1J(PtC) = 709 Hz, μ-***C***O]; $\delta(^{31}P)$ = 53.2 [s, ^1J(PtP) = 4814 Hz, ^2J(PtP) = 527 Hz, ^3J(PP) = 64 Hz, dppe]. NMR in CD_2Cl_2 at −90 °C: $\delta(^1H)$ = 4.35 [s, br, 12H, C***H₂***C***H₂*** of μ-dppe]; $\delta(^{13}C)$ = 250.6 [quintet, 1:8:18:8:1, ^1J(PtC) = 697 Hz, μ-***C***O]; $\delta(^{31}P)$ = 55.0 [s, ^1J(PtP) = 4796 Hz, ^2J(PtP) = 516 Hz, ^3J(PP) = 64 Hz, dppe].

$[Pt_6(\mu\text{-}CO)_6(\mu\text{-}dppp)_2(dppp)_2]$, 9. To a solution of $[PtCl_2(Me_2S)_2]$ (238 mg, 0.610 mmol) in THF (80 mL) was added dppp (168 mg, 0.407 mmol). The mixture was then treated with CO and $NaBH_4$ (323 mg) as above. The color of the solution changed through green, dark green, black, and finally to red. After 8 h of stirring under CO, MeOH (20 mL) was added, the solution was allowed to stir overnight under CO, the solvent was evaporated, and the brown-red solid was extracted with CH_2Cl_2. The dark-red solution was filtered through Celite and the solvent evaporated under vacuum to give the product as a brown-red solid in 85% yield. Anal. Calcd for $C_{114}H_{104}O_6P_8Pt_6$: C, 45.8; H, 3.5. Found: C, 45.7; H, 3.5. IR (Nujol): ν(CO) = 1835 (m), 1783 (vs, sh), 1772 (vs, sh), 1761 (vs) cm^{-1}. NMR in CD_2Cl_2 at 22 °C: $\delta(^1H)$ = 3.41 [s, br, 8H, ^3J(PtH) = 51 Hz, C***H₂***^{a}CH₂C***H₂***^{a} of μ-dppp], 3.09 [s, br, 4H, CH₂C***H₂***^{b}CH₂ of dppp], 2.66 [s, br, 8H, ^3J(PtH) = 50 Hz, C***H₂***^{c}CH₂C***H₂***^{c} of chelating dppp], 1.96 [s, br, 4H, CH₂C***H₂***^{d}CH₂ of dppp]; $\delta(^{13}C)$ = 256.1 [quintet, 1:8:18:8:1, $^1J(Pt^2C^2)$ = 791 Hz, μ-***C***O], 233.2 [quintet of triplet, 1:8:18:8:1, $^1J(Pt^2C^1)$ = 790 Hz, $^1J(Pt^1C^1)$ = 628 Hz, $^2J(Pt^2C)$ = 24 Hz, μ-***C***O]; $\delta(^{31}P)$ = 56.5 [t, P^b, $^1J(Pt^2P^b)$ = 4682 Hz, $^2J(Pt^1P^b)$ = 534 Hz, $^2J(Pt^2P^b)$ = 445 Hz, $^3J(P^bP^{b'})$ = 60 Hz, $^3J(P^aP^b)$ = 19 Hz], 25.5 [t, P^a, $^1J(Pt^1P^a)$ = 3425 Hz, $^2J(Pt^2P^a)$ = 294 Hz, $^3J(P^aP^b)$ = 19 Hz]; $\delta(^{195}Pt)$ = −2220 [tm, Pt^1, $^1J(Pt^1P^a)$ = 3425 Hz, $^2J(Pt^1P^b)$ = 536 Hz, $^1J(Pt^1Pt^2)$ = 386

(17) Hallam, M. F.; Mingos, D. M. P.; Adatia, T.; McPartlin, M. *J. Chem. Soc., Dalton Trans.* **1988**, 335.

(18) Roulet, R.; Barbey, C. *Helv. Chim. Acta* **1973**, *56*, 2179.

Hz], −2424 [tm, Pt^2, $^1J(Pt^2P^b) = 4682$ Hz, $^2J(Pt^2P^{b'}) = 445$ Hz, $^2J(Pt^2P^a) = 290$ Hz, $^1J(Pt^1Pt^2) = 386$ Hz]. NMR in CD_2Cl_2 at −90 °C: $\delta(^1H)$ showed five broad and overlapped resonances at 3.82, 2.92, 2.78, 2.15, and 2.07; $\delta(^{31}P) = 57.6$ [s, br, P^c, $^1J(Pt^2P^c) = 4562$ Hz, $^2J(Pt^1P^c) = 476$ Hz], 32.3 [s, br, P^a, $^1J(Pt^1P^a) = 3618$ Hz, $^2J(Pt^2P^a) = 362$ Hz], 23.1 [s, br, P^b, $^1J(Pt^1P^b) = 3230$ Hz, $^2J(Pt^2P^b) = 206$ Hz].

$[Pt_6(\mu_3\text{-}AuPPh_3)_2(\mu\text{-}CO)_6(\mu\text{-}dppe)_3][PF_6]_2$, 13. This cluster was synthesized by reaction of $[Pt_6(\mu\text{-}CO)_6(\mu\text{-}dppe)_3]$ (0.3 mmol) in CH_2Cl_2 (10 mL) with Ph_3PAuPF_6 (0.6 mmol) in THF (10 mL). The dark-green crystalline product **13** was obtained in 46% yield. Well-shaped black crystals could be obtained from CH_2Cl_2/diethyl ether. Anal. Calcd for $C_{120}H_{102}Au_2F_{12}O_6P_{10}Pt_6$: C, 38.5; H, 2.75. Found: C, 38.7; H, 2.5. IR (Nujol): ν(CO) = 1833 (vs) cm^{-1}. NMR in CD_2Cl_2 at 22 °C: $\delta(^1H) = 3.06$ [s, br, C***H*****$_2$**C***H*****$_2$** of μ-dppe]; $\delta(^{31}P) = 67.2$ [s, br, PPh_3], 44.8 [m, br, $^1J(PtP) = 4844$ Hz, dppe]. NMR in CD_2Cl_2 at −90 °C: $\delta(^{31}P) = 70.0$ [quintet, 1:4:7:4:1, $^2J(PtP) = 272$ Hz, PPh_3], 45.7 [s, $^1J(PtP) = 4792$ Hz, $^2J(PtP) = 320$ Hz, dppe].

Reaction of $[Pt_6(\mu\text{-}CO)_6(\mu\text{-}dppp)_2(dppp)_2]$ with Ph_3PAuPF_6. The reaction was conducted as above, but a complex mixture of products was formed.

$[Pt_6(\mu_6\text{-}Hg)(\mu\text{-}CO)_6(\mu\text{-}dppp)_3]$, 10a. To a solution of **9** (65 mg, 0.025 mmol) in CH_2Cl_2 (30 mL) was added excess mercury (1 drop). After 24 h of stirring, a black-green solution was obtained. The solution was filtered to remove unreacted mercury, and the product was obtained by evaporation of the solvent. It was purified by washing with acetone (0.5 mL) and diethyl ether (6 mL). Yield: 75%. Well-shaped black-green crystals could be obtained from CH_2Cl_2/diethyl ether or $ClCH_2CH_2Cl$/diethyl ether. Anal. Calcd for $C_{87}H_{78}HgO_6P_6Pt_6$: C, 37.6; H, 2.8. Found: C, 38.1; H, 2.9. EDX: Pt:Hg = 6:1. IR (Nujol): ν(CO) = 1837 (s), 1799 (vs), 1782 (vs) cm^{-1}. NMR in CD_2Cl_2 at 22 °C: $\delta(^1H) = 2.94$ [s, br, 12H, $^3J(PtH) = 52$ Hz, C***H*****$_2^a$**CH_2C***H*****$_2^a$** of dppp], 2.37 [s, br, 6H, CH_2C***H*****$_2^b$**CH_2 of dppp]; $\delta(^{13}C) = 235.1$ [quintet of triplet, 1:8:18:8:1, $^1J(PtC) = 714$ Hz, $^2J(PtC) = 41$ Hz, $^3J(PtC) = 22$ Hz, $^2J(HgC) = 75$ Hz, ***C***O]; $\delta(^{31}P) = 58.6$ [s, $^1J(PtP) = 5037$ Hz, $^2J(PtP) = 403$ Hz, $^2J(HgP) = 41$ Hz, $^3J(PP) = 55$ Hz, μ-dppp]; $\delta(^{195}Pt) = -2532$ [dm, $^1J(PtP) = 5037$ Hz, $^2J(PtP) = 403$ Hz, $^2J(HgPt) = 3350$ Hz, $^1J(PtPt) = 2200$ Hz, $^2J(PtPt) = 100$ Hz].

$[Pt_6(\mu_6\text{-}Tl)(\mu\text{-}CO)_6(\mu\text{-}dppp)_3][PF_6]$, 11a[$PF_6$]. To a solution of **9** (47 mg, 0.018 mmol) in CH_2Cl_2 (20 mL) was added $TlPF_6$ (6.4 mg). The red solution changed to dark green immediately. After 8 h of stirring, the solution was filtered and the solvent was removed under vacuum. The crude product was recrystallized from CH_2Cl_2/diethyl ether and washed with diethyl ether (6 mL) to give the pure product as a blue powder in 82% yield. Anal. Calcd for $C_{87}H_{78}F_6O_6P_7Pt_6Tl$: C, 35.7; H, 2.7. Found: C, 35.4; H, 2.8. EDX: Pt:Tl = 6:1. IR (Nujol): ν(CO) = 1871 (m), 1818 (vs, br) cm^{-1}. NMR in CD_2Cl_2 at 22 °C: $\delta(^1H) = 3.05$ [s, br, 12H, $^3J(PtH) = 53$ Hz, C***H*****$_2^a$**CH_2C***H*****$_2^a$** of dppp], 2.23 [s, br, 6H, CH_2C***H*****$_2^b$**CH_2 of dppp]; $\delta(^{13}C) = 232.5$ [quintet, 1:8:18:8:1, $^1J(PtC) = 696$ Hz, ***C***O]; $\delta(^{31}P) = 56.7$ [d, $^1J(PtP) = 4808$ Hz, $^2J(PtP) = 360$ Hz, $^2J(TlP) = 335$ Hz, μ-dppp].

$[Pt_6(\mu_6\text{-}Tl)(\mu\text{-}CO)_6(\mu\text{-}dppp)_3][BPh_4]$, 11a[$BPh_4$]. To a solution of **11a[PF_6]** (105 mg, 0.036 mmol) in a mixture of CH_2Cl_2/acetone (5 mL, ratio 1:2) was added a solution of $NaBPh_4$ (74 mg, 0.215 mmol) in methanol (5 mL). The green precipitate of the product which formed immediately was collected by filtration and washed with methanol (1 mL) and ether (5 mL). Yield: 84%. Well-shaped crystals could be obtained from CH_2Cl_2/diethyl ether. Anal. Calcd for $C_{111}H_{98}BO_6P_6Pt_6Tl$: C, 43.0; H, 3.2. Found: C, 43.3; H, 3.4. IR (Nujol): ν(CO) = 1870 (m), 1825 (vs, br) cm^{-1}. The NMR spectroscopic data are the same as for **11a[PF_6]**.

$[Pt_6(\mu_6\text{-}Tl)(\mu\text{-}CO)_6(\mu\text{-}dppp)_3][AsF_6]$, 11a[$AsF_6$]. The same procedure was followed as above with the use of $KAsF_6$ instead of $NaBPh_4$, to give the product as a black-green solid. Yield: 71%. Anal. Calcd for $C_{87}H_{78}AsF_6O_6P_6Pt_6Tl$: C, 35.2; H, 2.65. Found: C, 35.0; H, 2.4. IR (Nujol): ν(CO) = 1888 (m), 1869 (m), 1838 (s, sh), 1815 (vs, br) cm^{-1}. The NMR data are the same as for **11a[PF_6]**.

Reaction of 10a with $TlPF_6$. To a solution of **10a** (45 mg, 0.016 mmol) in CD_2Cl_2 (0.5 mL) was added $TlPF_6$ (5.7 mg). The yellow-green solution turned to blue over several hours. The reaction took ca. 1 day to complete as monitored by ^{31}P NMR spectroscopy. The analogous reaction of **11a**[PF_6] with Hg gave no detectable reaction over a period of 8 h as monitored by ^{31}P NMR spectroscopy, and only slow decomposition occurred over 2 days.

$[Pt_6(\mu_6\text{-}Hg)(\mu\text{-}CO)_6(\mu\text{-}dppb)_3]$, 10b. To a solution of $[PtCl_2(Me_2S)_2]$ (192 mg, 0.492 mmol) in THF (90 mL) was added dppb (105 mg). The solution was saturated with CO, and then $NaBH_4$ (260 mg) was added to the stirred solution. The color of the solution changed slowly to yellow-brown, then brown, and finally red in ca. 1 h. After 8 h of stirring under CO, MeOH (20 mL) was added and the solution was stirred overnight under a CO atmosphere. Excess mercury (8 drops) was added to the dark-red solution, and the color changed to yellow-green. The mixture was stirred for another 48 h under CO. The solvent was then evaporated under vacuum, and the residue was extracted with CH_2Cl_2 (20 mL × 8), the solution was filtered through Celite to give a yellow-green solution, and the solvent was evaporated under vacuum to give the product as a yellow-green solid in 76% yield. Well-shaped crystals could be obtained from CH_2Cl_2/diethyl ether. Anal. Calcd for $C_{90}H_{84}HgO_6P_6Pt_6$: C, 38.35; H, 3.0. Found: C, 39.1; H, 3.2. EDX: Pt:Hg = 6:1. IR (Nujol): ν(CO) = 1864 (s), 1828 (s), 1802 (s), 1791 (s, sh), 1778 (s, sh) cm^{-1}. NMR in CD_2Cl_2 at 22 °C: $\delta(^1H) = 2.93$ [s, br, 12H, $^3J(PtH) = 55$ Hz, C***H*****$_2^a$**CH_2bCH_2-bC***H*****$_2^a$** of μ-dppb], 2.18 [s, br, 12H, CH_2^aC***H*****$_2^b$**C***H*****$_2^b$**CH_2^a of μ-dppb]; $\delta(^{13}C) = 238.0$ [m, $^1J(PtC) = 715$ Hz, $2J(PtC) = 41$ Hz, μ-***C***O]; $\delta(^{31}P) = 46.6$ [s, $^1J(PtP) = 4919$ Hz, $^2J(PtP) = 396$ Hz, $^3J(PP) = 56$ Hz, $^2J(HgP) = 56$ Hz, $^1J(PtPt) = 1500$ Hz, $^1J(PtHg) = 3100$ Hz, dppb].

$[Pt_6(\mu_6\text{-}Tl)(\mu\text{-}CO)_6(\mu\text{-}dppb)_3][PF_6]$, 11b. The same procedure as above was followed with the use of 1 equiv $TlPF_6$ instead of excess mercury. The green product was isolated in 78% yield. Anal. Calcd for $C_{90}H_{84}F_6O_6P_7Pt_6Tl$: C, 34.1; H, 2.7. Found: C, 33.5; H, 2.3. IR: ν(CO) = 1808 (s), 1776 (s) cm^{-1}. NMR in CD_2Cl_2: $\delta(^{31}P) = 47$ [v br, $^1J(PtP) = 5050$ Hz, dppb].

$[Pt_6(\mu_6\text{-}Hg)(\mu\text{-}CO)_6(CO)_2(\mu\text{-}dpppe)_2]$, 12a. The same procedure was followed as above with the use of ligand dpppe instead of dppb. The product obtained is a green solid, which contained ca. 5% impurity of **10c**, in 76% yield. IR: ν(CO) = 2030 (m), terminal CO, 1826 (m), 1794 (s), bridging CO. NMR in CD_2Cl_2: $\delta(^{13}C) = 196$ [m, $^1J(PtC) = 2295$ Hz, $^2J(PtC) = 126$ Hz, t-CO]; 225 [m, $^1J(PtC) = 886$, 595 Hz, μ-CO]; 235 [m, $^1J(PtC) = 735$ Hz, μ-CO]. $\delta(^{31}P) = 50.2$ [s, $^1J(PtP) = 4960$ Hz, $^2J(Pt^1P) = 447$ Hz, $^2J(Pt^2P) = 371$ Hz, $^3J(PP) = 46$ Hz, dpppe]; $\delta(^{195}Pt) = -2324$ [m, $^1J(Pt^1Pt^2) = 2225$ Hz, $^2J(Pt^1P) = 447$ Hz, Pt^1]; Pt^2 resonance not observed.

$[Pt_6(\mu_6\text{-}Hg)(\mu\text{-}CO)_6(\mu\text{-}dpppe)_3]$, 10c. To a solution of **12a** (79 mg, 0.031 mmol) in CH_2Cl_2 (20 mL) was added dpppe (0.035 mmol). The green solution turned to yellow-green immediately. After 0.5 h of stirring, the solvent was removed to obtain a green solid which was recrystallized from CH_2Cl_2/hexane to give the product as an green solid in 82% yield. Anal. Calcd for $C_{93}H_{90}O_6P_6Pt_6Hg$: C, 39.05; H, 3.2. Found: C, 39.4; H, 3.3. EDX: Pt:Hg = 6:1. IR (Nujol): ν(CO) = 1830 (m), 1788 (vs) cm^{-1}. NMR in CD_2Cl_2 at 22 °C: $\delta(^1H) = 3.02$ [s, br, 12H, $^3J(PtH) = 53$ Hz, C***H*****$_2^a$**$CH_2^b$$CH_2^c$$CH_2^b$C***H*****$_2^a$** of μ-dpppe], 2.04 [s, br, 12H, CH_2^aC***H*****$_2^b$**CH_2^cC***H*****$_2^b$**CH_2^a of μ-dpppe], 1.53 [s, br, 6H, $CH_2^a$$CH_2^b$C***H*****$_2^c$**$CH_2^b$$CH_2^a$ of μ-dpppe]; $\delta(^{13}C) = 235$ [$^1J(PtC) = 720$ Hz, μ-CO]; $\delta(^{31}P) = 53.2$ [s, $^1J(PtP) = 4980$ Hz, $^2J(PtP) = 403$ Hz, $^3J(PP) = 55$ Hz, $^2J(HgP) = 76$ Hz, dpppe]; $\delta(^{195}Pt) = -2497$ [m, $^1J(PtP) = 4980$ Hz, $^2J(PtP) = 400$ Hz].

$[Pt_6(\mu_6\text{-}Hg)(\mu\text{-}CO)_6(CO)_2(\mu\text{-}dpph)_2]$, 12b. The same procedure was followed as for **2a** with the use of ligand dpph instead of dpppe. The product was obtained as a green solid, containing the impurity of **10d**. The yield of **12b** is ca. 30%

yield (based on the integration of the ^{31}P NMR spectra). IR: ν(CO) = 2030 (m), terminal CO; 1830 (m), 1790 (s), bridging CO. NMR in CD_2Cl_2: $\delta(^{13}C)$ = 196 [m, ^1J(PtC) = 2160 Hz, ^2J(PtC) = 125 Hz, ^3J(PC) = 16 Hz, t-CO]; 225 [m, ^1J(PtC) = 860, 540 Hz, μ-CO]; 235 [m, ^1J(PtC) = 705 Hz, μ-CO]; $\delta(^{31}P)$ = 49.2 [s, ^1J(PtP) = 4975 Hz, $^2J(Pt^1P)$ = 430 Hz, $^2J(Pt^2P)$ = 370 Hz, ^3J(PP) = 50 Hz, dpppe]; $\delta(^{195}Pt)$ = −2271 [m, $^1J(Pt^1Pt^2)$ = 2070 Hz, $^2J(Pt^1P)$ = 460 Hz, Pt^1]; −2695 [br, ^1J(PtP) = 5100 Hz, Pt^2].

[Pt$_6$(μ_6-Hg)(μ-CO)$_6$(μ-dpph)$_3$], 10d. The same procedure as for **10c** was followed. The product was obtained as a green solid in 84% yield. Anal. Calcd for $C_{96}H_{96}HgO_6P_6Pt_6$: C, 39.7; H, 3.3. Found: C, 39.9; H, 3.7. EDX: Pt:Hg = 6:1. IR (Nujol): ν(CO) = 1823 (m), 1781 (vs) cm^{-1}. NMR in CD_2Cl_2 at 22 °C: $\delta(^1H)$ = 3.25 [s, br, 12H, C$\boldsymbol{H_2^a}$CH_2^bCH_2^cCH_2^c-CH_2^bC$\boldsymbol{H_2^a}$ of μ-dpph], 2.15 [s, br, 24H, CH_2^aC$\boldsymbol{H_2^b}$C$\boldsymbol{H_2^c}$C$\boldsymbol{H_2^c}$C$\boldsymbol{H_2^b}$-CH_2^a of μ-dpph]; $\delta(^{13}C)$ = 232.7 [quintet, 1:8:18:8:1, ^1J(PtC) = 744 Hz, ***C***O]; $\delta(^{31}P)$ = 52.9 [s, ^1J(PtP) = 4961 Hz, ^2J(PtP) = 397 Hz, ^3J(PP) = 56 Hz, ^2J(HgP) = 70 Hz, dpph]; $\delta(^{195}Pt)$ = −2476 [m, ^1J(PtP) = 4960 Hz, ^2J(PtP) = 400 Hz, ^1J(PtPt) = 2100 Hz, ^1J(PtHg) = 3100 Hz].

Details of the X-ray Structure Determination. Very dark crystals (small crystals are green by reflected light but red by transmitted light) of **11a**[BPh_4] were grown from CH_2Cl_2/ether by slow diffusion at room temperature. After many attempts with weakly diffracting crystals, a suitable crystal fragment with dimensions 0.35 × 0.25 × 0.20 mm was mounted inside a Lindemann capillary tube and flame sealed. The diffraction experiments were carried out using a Siemens P4 diffractometer with XSCANS software package[19] using graphite monochromated Mo Kα radiation at 23 °C. The cell constants were obtained by centering 25 reflections (15.4 ≤ 2θ ≤ 25°). The Laue symmetry was determined by merging symmetry equivalent reflections. The data were collected in shells, in the θ range 2.0−21° (−1 ≤ h ≤ 16, −1 ≤ k ≤ 26, −27 ≤ l ≤ 27) in ω scan mode at variable scan speeds (2−20 deg/min). Background measurements were made at the ends of the scan range. Four standard reflections were monitored at the end of every 297 reflection collection. It was found that the data crystal was very unstable to X-rays and the intensity of the standards fell during the data collection (correction factors: minimum, 0.547; mean, 0.851). The data collection was therefore stopped near the θ_{max} of 21°. At the end of the data collection, the faces of the data crystal were indexed, and the distances between the faces were measured. A Gaussian absorption correction was applied to the data (μ = 8.635 mm^{-1}). The maximum and minimum transmission factors are 0.2868 and 0.1629, respectively. The space group $P2_1/n$ was determined from the systematic absences. The data processing, solution, and initial refinements were done using SHELXTL-PC programs.[20] The final refinements were performed using SHELXL-93 software programs.[21] Anisotropic thermal parameters were refined for all the platinum, thallium, phosphorus, and chlorine atoms. The rest of the atoms were refined isotropically. The phenyl rings were treated like ideal hexagons with C−C = 1.395 Å. The dichloromethane solvent was found to occupy two different positions in the crystal lattice with occupancies 0.6/0.4. Soft constraints were applied for the distances with similar C−Cl, B−C, and aliphatic C−C bonds using SADI. No attempt was made to locate the hydrogen atoms. However all the hydrogen atoms were placed in the calculated positions in the cation and their isotropic thermal parameters were assigned 20% more than the atoms they are attached to. In the final least-squares refinement cycles on F^2, the model converged at $R1$ = 0.0999, w$R2$ = 0.2312, and Goof = 1.000 for 4825 observations with $_F$o ≥ 4$\sigma(F_o)$ and 443 parameters and $R1$ = 0.2652 and w$R2$ = 0.3336 for all 12 440 data. Poor agreement factors are attributed to weak reflections caused by crystal decay. In the final difference Fourier synthesis the electron density fluctuates in the range 2.13 to −2.34 e Å^{-3} . Most of peaks in the difference Fourier map were found near the heavy atoms. The mean and the maximum shift/esd values in the final cycles were 0.004 and −0.040. The experimental details and crystal data are in Table 4. Positional and thermal parameters, complete bond distances and angles, anisotropic thermal parameters, hydrogen atom coordinates, and selected torsion angles have been included in the Supporting Information.

Table 4. Crystal Data and Experimental Details for 11a[BPh_4]

formula	$C_{112}H_{100}BCl_2O_6P_6Pt_6Tl$
fw	3184.36
temperature	23 °C
wavelength	0.710 73 Å
cryst system	monoclinic
space group	$P2_1/n$
cell dimens	a = 16.571(4) Å b = 26.030(6) Å c = 27.447(6) Å β = 95.80(2)°
cell vol, Z	11778(4) Å^3, 4
density: calcd, obsd	1.796, 1.90(5) g·cm^{-3}
abs coeff	8.635 mm^{-1}
data/restraints/params	12440/61/443
goodness-of-fit (GooF)[a] on F^2	1.000
final R indices [$I > 2\sigma(I)$][a]	$R1$ = 0.0999, w$R2$ = 0.2312

[a] $R1 = \sum(||F_o| - |F_c||)/\sum|F_o|$; w$R2 = [\sum w(F_o^2 - F_c^2)^2/\sum wF_o^4]^{1/2}$; GooF $= [\sum w(F_o^2 - F_c^2)^2/(n - p)]^{1/2}$, where n is the number of reflections and p is the number of parameters refined.

Acknowledgment. We thank the NSERC (Canada) for financial support.

Supporting Information Available: Tables of data collection parameters, atomic coordinates, thermal parameters, and bond distances and angles (14 pages). Ordering information is given on any current masthead page.

OM960148K

(19) XSCANS, Siemens Analytical X-Ray Instruments Inc., Madison, WI. 1990.

(20) Sheldrick, G. M. SHELXTL-PC Software, Siemens Analytical X-Ray Instruments Inc., Madison, WI, 1990.

(21) Sheldrick, G. M. SHELXL-93, Institut fur Anorg. Chem., Goettingen, Germany, 1993.